Hindawi
Journal of Chemistry
Volume 2024, Article ID 9848962, 1 page
https://doi.org/10.1155/2024/9848962

Retraction

Retracted: Simulation of the Electro-Superconducting System Based on the H Equation

Journal of Chemistry

Received 23 January 2024; Accepted 23 January 2024; Published 24 January 2024

This article has been retracted by Hindawi following an investigation undertaken by the publisher [1]. This investigation has uncovered evidence of one or more of the following indicators of systematic manipulation of the publication process:

(1) Discrepancies in scope

(2) Discrepancies in the description of the research reported

(3) Discrepancies between the availability of data and the research described

(4) Inappropriate citations

(5) Incoherent, meaningless and/or irrelevant content included in the article

(6) Manipulated or compromised peer review

The presence of these indicators undermines our confidence in the integrity of the article's content and we cannot, therefore, vouch for its reliability. Please note that this notice is intended solely to alert readers that the content of this article is unreliable. We have not investigated whether authors were aware of or involved in the systematic manipulation of the publication process.

Wiley and Hindawi regrets that the usual quality checks did not identify these issues before publication and have since put additional measures in place to safeguard research integrity.

We wish to credit our own Research Integrity and Research Publishing teams and anonymous and named external researchers and research integrity experts for contributing to this investigation.

The corresponding author, as the representative of all authors, has been given the opportunity to register their agreement or disagreement to this retraction. We have kept a record of any response received.

References

[1] J. Zhang, "Simulation of the Electro-Superconducting System Based on the H Equation," *Journal of Chemistry*, vol. 2022, Article ID 6831771, 7 pages, 2022.

Hindawi
Journal of Chemistry
Volume 2022, Article ID 6831771, 7 pages
https://doi.org/10.1155/2022/6831771

Research Article

Simulation of the Electro-Superconducting System Based on the H Equation

Jun Zhang

College of Computer and Information Engineering, Guizhou University of Commerce, Guiyang 550014, Guizhou, China

Correspondence should be addressed to Jun Zhang; 202007000289@hceb.edu.cn

Received 9 April 2022; Revised 31 May 2022; Accepted 6 June 2022; Published 2 July 2022

Academic Editor: Ajay Rakkesh R

In order to reduce the levitation energy consumption and increase the levitation air gap, a simulation study of the electrochemistry superconducting magnetic levitation system based on the H equation is proposed. Through finite element simulation, the magnetic field distribution, current distribution, force, and other characteristics of the magnetic suspension system in the superconducting gravimeter are obtained; the relationship between the force of the superconducting ball in the magnetic field and the height of the suspension body and the current of the suspension coil is analyzed; and the penetration rate, the magnetic gradient, penetration depth, and maximum magnetic induction intensity of the superconducting spherical surface of the single-coil electrochemistry superconducting magnetic levitation system are obtained by simulation calculation. Simulation results show that, at 1 s, we start to use 0.2 s, 0.4 s, 0.6 s, and 0.8 s time, respectively, to pass current into the floating coil until it reaches 4.4 A. The magnetic gradient of the electrochemistry superconducting magnetic levitation system using a single coil is too large to meet the requirements of gravity measurement, the penetration depth is much smaller than the thickness of the superconducting sphere, and the maximum magnetic field on the surface of the superconducting sphere is much smaller than the critical magnetic field value of the superconducting material, and no loss will occur. The critical magnetic field value of the superconducting sphere is much smaller than that of the superconducting sphere. The critical magnetic field value of the material will not quench, which verifies that the H equation can simulate the superconducting magnetic levitation system well and has a high simulation accuracy and efficiency.

1. Introduction

With the continuous development of society, the future development trend of rail transit will have the characteristics of energy saving, environmental protection, safety and comfort, fast, and convenience. In addition to technological innovations in existing rail transportation vehicles, rail transit in the twenty-first century, it is also necessary to vigorously develop new rail transportation vehicles, and the maglev train was born [1]. At the same time, with the continuous development of superconducting materials, combining superconducting materials and magnetic levitation trains makes the maglev train faster, develops operational reliability, high safety, low loss and noise, and is comfortable and environmentally friendly [2]. According to its working principle and technical characteristics, traditional maglev trains can be divided into electromagnetic attraction type (EMS) and electrodynamic repulsion type (EDS) [3]. Electromagnetic attraction (EMS) maglev trains mainly use electromagnets installed on the bogies on both sides of the train and magnets laid on the rails of the line; the attractive force generated under the action of a magnetic field attracts the long stator core under the guide rails to make the train levitate; the magnets on both sides of the guide rail and the magnets on both sides of the train generate attractive force to achieve guiding and braking functions [4, 5].

At present, conventional gravimeters mainly use mechanical springs to achieve the suspension of inspection quality. In the long-term measurement process, mechanical springs will have problems such as creep, hysteresis, and nonlinearity, and as a result, the accuracy of gravity measurement continues to decrease. With the continuous development of low temperature and superconducting

technology, it has become possible to apply superconducting magnetic levitation technology to gravity measurement. The superconducting gravimeter utilizes the zero resistance and Meissner characteristics of the superconductor, which can make the superconductor stably suspended in the magnetic field without energy loss. Since the system is working at low temperature, the thermal noise and expansion coefficient of the system are greatly reduced; this makes the superconducting gravimeter have extremely high measurement accuracy, very low noise, and drift rate, and it can solve a series of problems existing in conventional mechanical gravimeters [6]. Moreover, for the simulation of the magnetic levitation system in the superconducting gravimeter, due to the need to obtain a large amount of simulation data to guide the experiment, the simplified A-equation static magnetic field model is usually used for simulation. We set the permeability of the superconducting sphere to 0 or set the surface of the niobium sphere as a magnetic insulation boundary condition; the virtual displacement method or the magnetic pressure formula can be used to quickly obtain the force and magnetic force gradient of the superconducting niobium ball in the magnetic field [7]. This method is an ideal model, unable to obtain the magnetic field and shielding current distribution inside the superconducting sphere; through our experiments, it is found that there is a large deviation from the simulation, which will lead to deviations in the design of the suspension system. The H equation based on the magnetic field strength is a new method for solving superconducting systems. There are few related studies at present; we apply it to the simulation of the magnetic levitation system in the superconducting gravimeter, and it can solve the magnetic field distribution, shielding current, force, and AC loss in the superconducting sphere; on the other hand, the H equation is easier to implement in the finite element software COMSOL, this can improve the simulation efficiency and accuracy of the magnetic levitation system in the superconducting gravimeter. Fujii et al. proposed a three-phase permanent magnet motor drive using only a three-phase inverter and a degree of freedom controlled magnetic levitation drive method. The suspension winding is connected between the neutral point of the Y-connected motor winding and the middle point of the voltage source. Therefore, the levitation force is actively controlled by the zero sequence current. The experimental results show that under the load state of the motor, the vibration of the magnetic suspension is increased compared to that under no load. Vibration mainly includes the driving frequency, the basic, and third components of 1F and 3F. We focus on the improvement of the positioning accuracy of the magnetic levitation system. We found that the vibration 1F is caused by the detection error of the current sensor and the three-phase unbalanced resistance and inductance, and the vibration 3F is caused by PWM driving. In order to improve positioning accuracy, we studied current detection methods and observer-based voltage disturbance compensation. Experimental results show that these compensations improve the positioning accuracy of magnetic levitation [8].

Based on this research, taking the magnetic levitation system in the superconducting gravimeter as the research object, we discussed the structure of the magnetic levitation system in the superconducting gravimeter, introduced the basic principles of H equation finite element simulation; the shielding current, magnetic field distribution, and levitation characteristics of the magnetic levitation system in the superconducting gravimeter are analyzed. The results are compared with experimental results and the A equation static magnetic field method, the error causes are analyzed. It lays a theoretical foundation for further improving the design precision of the superconducting gravimeter and also provides a certain reference significance for improving the simulation efficiency and precision of the superconducting system.

2. Research Methods

2.1. The Structure of the Superconducting Magnetic Levitation System Applied to Gravity Measurement. A typical application of the superconducting magnetic levitation system is a superconducting gravimeter [9]. In a low temperature environment, utilizing the zero resistance characteristics of superconductors can produce unchanged current in the superconducting coil; this produces a very stable background magnetic field. We place a high-precision superconducting niobium ball in the background magnetic field, and the Meissner effect of superconductors can equivalently act as a "spring" in a mechanical gravimeter, the superconducting ball is forced and suspended. Because it does not use mechanical springs and works in a 4.2 K liquid helium environment, the superconducting gravimeter can achieve extremely high measurement accuracy, very low noise, and drift rate [10]. The structure of the superconducting magnetic levitation system for gravity measurement is mainly composed of a superconducting levitation coil, a superconducting niobium ball, and a displacement detection capacitor. The superconducting ball floats under the Meissner effect and the suspension force and gravity reach a balance; by adjusting the current in the upper and lower superconducting coils, the magnetic force gradient in the space area can be adjusted, that is, the stiffness of the "spring". When the gravity changes slightly, the superconducting ball will be displaced in the vertical direction, reach a new equilibrium position, so the distance between the upper and lower capacitor plates will change, and the measurement of gravity can be completed by the differential capacitance detection circuit [11].

2.2. The Basic Principle of the H Equation Finite Element Simulation. A two-dimensional rotational axis symmetric transient field model is used to model the superconducting Maglev system for gravity measurement. From Faraday's law of electromagnetic induction and the B-H constitutive relationship, the following equation can be obtained:

$$\nabla \times \vec{E} = -\frac{\partial \vec{B}}{\partial t} = -\mu_0 \frac{\partial \left(\mu_r \vec{H}\right)}{\partial t}. \quad (1)$$

In the formula, μ_0, μ_r are the vacuum permeability and the relative permeability of the material, respectively, for

superconductors, take its relative permeability $\mu_r = 1$, the shield current model is used to describe its superconductivity. In a two-dimensional rotational axisymmetric model, we use the cylindrical coordinate system (r, z, φ); since the current flowing into the floating coil only has a circular component, therefore, there are only H_r, H_z, E_φ, J_φ components in the spatial region. The curl vector equation (1) can be decomposed into two scalar equations in the r and z directions as shown in fd2:

$$\begin{bmatrix} -\dfrac{\partial E_\varphi}{\partial_z} \\ \dfrac{E_\varphi}{r} + \dfrac{\partial E_\varphi}{\partial r} \end{bmatrix} = -\mu_0 \frac{\partial}{\partial t} \begin{bmatrix} \mu_r H_r \\ \mu_r H_z \end{bmatrix}. \tag{2}$$

For nonsuperconducting regions, Ohm's law $E_\varphi = \rho J_\varphi$, where ρ is the resistivity of the material; for the superconducting region, using the classic E-J equation to describe the nonlinear constitutive relationship in the second type of superconductor, we obtain as follows:

$$E = E_0 \left(\frac{J}{J_c} \right)^n. \tag{3}$$

Among them, E_0 is the critical electric field strength, n is a constant, and both affect the speed of the superconductor's zero resistivity transition, determined by the superconducting material, $E_0 = 0.0001\,V/m, n = 21$ is selected in this simulation.

J_c is the critical current density of the superconductor, susceptible to external magnetic field and temperature; the classic Kim model is used to describe the relationship between the critical current density and the external magnetic field as follows:

$$J_c(B) = \frac{J_{c0}}{\left(1 + \left|\mu_0 \mu_r H / B_0\right|\right)^\alpha}. \tag{4}$$

Among them, J_{c0} is the critical current density of the superconductor when the external magnetic field is zero, B_0 is the superconducting material parameter, and α is the Kim coefficient. Since the superconducting magnetic levitation system of this model is in a 4.2 K constant temperature liquid helium environment, and the magnetic field used for levitation changes very little; therefore, the influence of external temperature and magnetic field changes on the critical current density of superconducting niobium spheres can be ignored; we take it as a fixed value. In this simulation, the critical current density is taken as $10^8\,A/m^2$.

From Ampere's loop law $\vec{J} = \nabla \times \vec{H}$, it can be obtained as follows:

$$J_\varphi = \frac{\partial H_r}{\partial z} - \frac{\partial H_z}{\partial r}. \tag{5}$$

Incorporating formulas (3) and (5) into formula (2), the governing equation of the superconducting region can be obtained as follows:

$$\begin{bmatrix} -\dfrac{\partial}{\partial z}\left(E_0 \left(\dfrac{\partial H_r/\partial z - \partial H_z/\partial r}{J_c} \right)^n \right) \\ \dfrac{1}{r} E_0 \left(\dfrac{\partial H_r/\partial z - \partial H_z/\partial r}{J_c} \right)^n + \dfrac{\partial}{\partial r} E_0 \left(\dfrac{\partial H_r/\partial z - \partial H_z/\partial r}{J_c} \right)^n \end{bmatrix} = -\mu_0 \frac{\partial}{\partial t} \begin{bmatrix} \mu_r H_r \\ \mu_r H_z \end{bmatrix}. \tag{6}$$

As for the nonsuperconducting area, we simply put Ohm's law and formula (5) into formula (2); thus, the governing equation of the magnetic field intensity H in the entire region is obtained. From the governing equations and boundary conditions, the H distribution in the entire spatial domain can be obtained, then we use the B–H constitutive relationship and formula (5) to obtain the magnetic field distribution and current distribution in space. Finally, the Lorentz force equation can be used to obtain the force of the superconducting sphere in the magnetic field as follows:

$$\vec{F} = \int_V \vec{J}_{sc} \times B \, dV. \tag{7}$$

Among them, J_{sc} is the shielding current density in the superconductor, B is the magnetic induction intensity, and V is the volume area of the superconductor.

Because COMSOL's "Magnetic Field Formula" interface can set material properties with obvious nonlinear E-J characteristics, the finite element simulation of the model can be performed in COMSOL. It should be noted that the "conduction current relationship" of the superconductor should be selected as the "E-J characteristic" and input into equation (3).

Another thing to note is that, in the process of finite element meshing, it is necessary to divide the mesh close to the surface of the superconductor to be particularly small; because according to the London equation, the magnetic field and shielding current only exist within a few angstroms to hundreds of angstroms on the surface of the superconductor and decay exponentially. After many simulations, it was found that if the mesh on the surface of the superconductor is too large, it will not be able to accurately reflect the magnetic field and shield current distribution on the superconductor or affect the accuracy of the solution; this is also difficult to achieve using MATLAB to write finite element programs [12].

2.3. The Principle and Classification of High-Temperature Superconducting Linear Motors. Introducing high-temperature superconducting materials into traditional linear motors, then combining with the diamagnetism of high-temperature superconducting materials, strong capture field characteristics, and self-suspension and self-direction characteristics, it laid a theoretical and technical foundation for the development of practical high-temperature superconducting linear motor technology. At present, many

countries have conducted in-depth research on high-temperature superconducting linear motor technology, through theoretical analysis, established related models, and developed a variety of prototypes. Among them, the more extensive research is the high-temperature superconducting linear synchronous motor, according to the different types of superconducting materials used and the different application principles, it is classified as follows: (1) High-temperature superconducting bulk magnet secondary linear synchronous motor; (2) primary linear synchronous motor with high-temperature superconducting coil; (3) high-temperature superconducting coil magnet secondary linear synchronous motor; (4) high-temperature superconducting block linear reluctance synchronous motor; and (5) full-superconducting high-temperature superconducting linear synchronous motor. According to its structural composition, it can be divided into 69–7: (1) unilateral type; (2) bilateral type; and (3) cylindrical type.

Different types of high-temperature superconducting linear synchronous motors have their practical application scenarios and advantages and disadvantages. The above types of high-temperature superconducting linear synchronous motors can be divided into semi-superconducting and full-superconducting types. Compared to the fully superconducting type, the semi-superconducting structure is simpler, less materials are used, the superconducting cooling system is simpler, and maintenance is simpler. The full-superconducting structure and cooling system are more complicated, but the thrust generated is greater and the efficiency is higher [13, 14]. For the unilateral type, the primary and secondary will produce a lot of normal force. In order to solve this problem, a two-sided structure can be used.

3. Result Analysis

In the actual process, both the superconducting niobium ball and the suspension coil are in a 4.2 K liquid helium environment. It is impossible to directly measure the force of a superconducting ball, only indirectly verifying the simulation results can be adopted. When the superconducting ball is in the middle position, the distance to the upper and lower capacitor plates is 0.5 mm. In the initial state, the ball falls on the lower capacitor plate due to gravity, with the gradual increase of the floating coil current, the suspension force of the ball is also gradually increasing; when the levitation force reaches the gravity of the ball, the ball starts to leave the lower capacitor plate to achieve magnetic levitation, and the suspension force of the superconducting ball in each suspension position is equal to the gravity of the ball [15]. The relationship between the floating height of a fixed-mass superconducting ball (gravity of 0.12828 N) and the current of the floating coil can be measured through experiments; in order to reduce the variable, only the lower coil current is passed. For simulation, the same structure size is used for modeling, the suspension height of the ball is adjusted, and different currents are applied to the levitation coil until the levitation force obtained by the simulation is equal to the gravity 0.1828 N. Figure 1 shows the relationship between

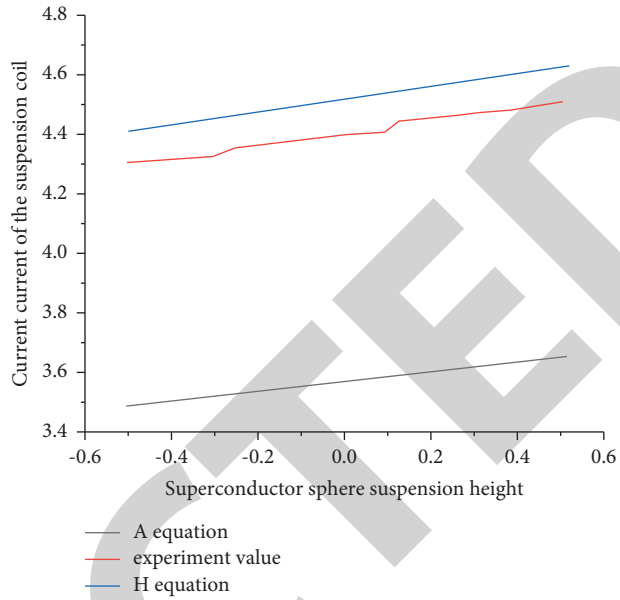

Figure 1: The relationship between the levitation height and coil current.

the floating height of the ball and the current of the floating coil obtained by the experiment and the simulation using the H equation, and it is compared with the data obtained from the static magnetic field model of Equation A.

As you can see from the figure, within −0.5 mm and 0.5 mm, the floating height obtained by experiment and simulation is basically linear with the coil current; but to suspend superconducting balls of the same mass at a certain height, the suspension current obtained by H equation simulation is more close to the actual current. It is only 2.7% higher than the actual current, which is very helpful for designing the suspension coil in the superconducting gravimeter. However, the current simulated by the static magnetic field model of Equation A is 23.6% lower than the actual value, this is mainly because under the same current, the ideal model with a permeability of 0 is used to calculate that the force on the superconductor is greater than the actual value, therefore, under the same height and force, the current required for simulation using the A-equation static magnetic field model is much smaller than the actual value. In contrast between the two, using the H equation simulation can indeed improve the simulation accuracy of the magnetic levitation system in the superconducting gravimeter [16, 17].

By bringing the floating height and current data obtained from the experiment into the H equation simulation model, it can simulate and calculate the suspension force of the ball as shown in Table 1. Compared with the actual force value 0.1828 N, it can be seen that the force calculated by the simulation of the H equation is only 6-7 mN lower than the actual force, the error is about 5%, within our tolerance range. The reason for the analysis error may be that our suspension coils are not wound uniformly and regularly, the machining, assembly, and measurement errors of superconducting niobium balls, and meshing during simulation,

Table 1: Suspension force obtained by the simulation.

Experiment through human coil current (A)	Experimentally measured floating position (mm)	Suspension force obtained by simulation (N)
4.3	−0.4	0.112115
4.34	−0.25891	0.111552
4.36	−0.18398	0.11217
4.38	−0.08524	0.11163
4.4	0.002501	0.111556
4.42	0.072633	0.111697
4.44	0.108347	0.112343
4.46	0.244902	0.111748
4.48	0.371653	0.111251
4.51	0.4	0.111674

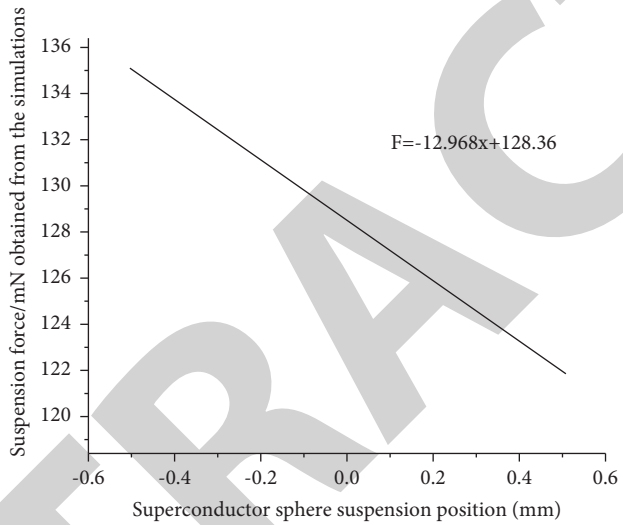

Figure 2: The relationship between the suspension force and the suspension position of the ball.

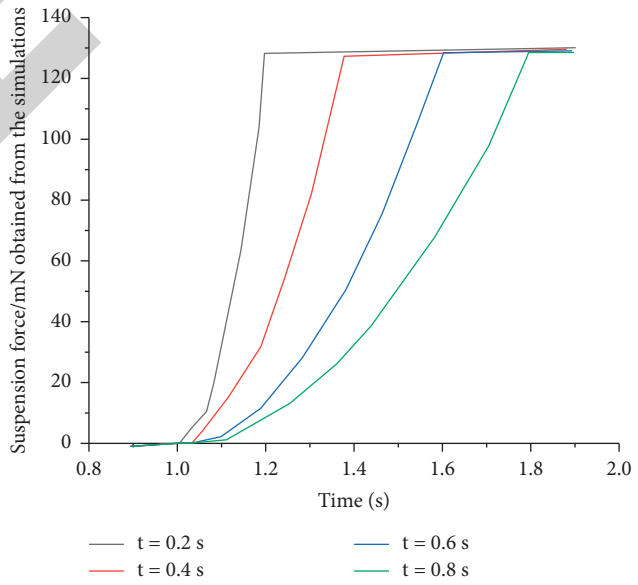

Figure 3: Levitation force obtained by applying current at different times.

the use of single-turn wire instead of the actual multiturn coil caused, in the future experiments and simulation process, we need to find ways to improve to further improve the simulation accuracy.

We fix the current when the superconducting ball is in the center position; by suspending the ball at different heights, the relationship between the levitation force and the levitation position of the ball can be simulated, as shown in Figure 2, so as to calculate the rigidity of the magnetic levitation system. As can be seen from the figure, in the range of −0.5–0.5 mm, the levitation force received by the ball is negatively related to the levitation height [18]. Through the levitation force-displacement curve, the magnetic force gradient of the system can be obtained, that is, the "spring" stiffness is about 12.968 N/m. Obviously, the use of a single-coil levitation system cannot meet the need for a small stiffness of 10−2 N/m in the superconducting gravimeter; a double-coil suspension system is needed to improve the design accuracy of the superconducting gravimeter.

Figure 3 shows the curve of the force of the superconducting ball obtained by simulation with time; at 1 s, we start to use 0.2 s, 0.4 s, 0.6 s, and 0.8 s time, respectively, we pass current into the floating coil until it reaches 4.4 A. It can be found from the figure that the rate of current flow only affects the rate of change of the force on the superconducting ball, but it does not affect the magnitude of the final force. When the magnitude of the applied current remains the same, the force on the ball no longer changes, but it is not necessarily zero, which is different from the force of a conventional conductor in a changing magnetic field. The results of experiment and simulation are basically the same.

Through the comparison of experiment and simulation, it is verified that the H equation can better simulate the superconducting magnetic levitation system, and it has higher simulation accuracy and efficiency [19]. Through finite element simulation, the magnetic field distribution of the magnetic levitation system in the superconducting gravimeter, current distribution, force, and other characteristics are obtained, the force and levitation height of the superconducting ball in the magnetic field are analyzed, and the current size of the floating coil, the rate of access, the simulation calculation has obtained the magnetic force gradient, the penetration depth, the maximum magnetic induction intensity on the surface of the superconducting sphere [20]. Simulation results show that the magnetic force gradient of the superconducting magnetic levitation system using a single coil is too large to meet the requirements of gravity measurement; the penetration depth is much smaller than the thickness of the superconducting ball, moreover, the maximum value of the magnetic field on the surface of the superconducting sphere is much smaller than the critical magnetic field value of the superconducting material, so quenching will not occur.

4. Conclusion

The current simulation of the magnetic levitation system in the superconducting gravimeter mainly adopts the A-equation static magnetic field method; the data obtained by simulation are quite different from the experimental results. In order to improve simulation accuracy and efficiency, a new simulation model was established in COMSOL using the H equation. The data obtained by simulation has a small deviation from the experimental results, and it is verified that this method can improve the simulation accuracy and efficiency of the superconducting magnetic levitation system. The simulation obtained the magnetic field distribution of the magnetic levitation system in the superconducting gravimeter, shielding current distribution, force, penetration depth, and other characteristics analyzed the levitation force and levitation height of the superconducting ball in the magnetic field. The relationship between the suspension force of superconducting balls in the magnetic field and the current passing rate of suspension coil at suspension height is analyzed. The magnetic gradient of the superconducting Maglev system is calculated. The rationality and correctness of the designed magnetic levitation system are verified.

Data Availability

The data used to support the findings of this study are available from the corresponding author upon request.

Conflicts of Interest

The authors declare that they have no conflicts of interest.

Acknowledgments

This study was supported by the Second Batch of New Engineering Research and Practice Projects (Project No.: EDXKJC20200524), Reform Items of Teaching Content and Curriculum System of Colleges and Universities in Guizhou Province in 2020 (Project No.: 2020141), and First class undergraduate major of Guizhou University of Commerce (Project No.: 2021YJZY01.)

References

[1] S. Suzuki and A. Satoh, "Influence of the cluster formation in a magnetic particle suspension on heat production effect in an alternating magnetic field," *Colloid and Polymer Science*, vol. 297, no. 10, pp. 1–9, 2019.

[2] S. Yook, S. S. Shams Es-haghi, A. Yildirim, Z. Mutlu, and M. Cakmak, "Anisotropic hydrogels formed by magnetically-oriented nanoclay suspensions for wound dressings," *Soft Matter*, vol. 15, no. 47, pp. 9733–9741, 2019.

[3] H. E. Mollabashi and A. H. Mazinan, "Incremental smc-based cnf control strategy considering magnetic ball suspension and inverted pendulum systems through cuckoo search-genetic optimization algorithm," *Complex & Intelligent Systems*, vol. 5, no. 3, pp. 353–362, 2019.

[4] X. Liu, G. Ying, X. Liao et al., "Cytometric microbead magnetic suspension array for high-throughput ultrasensitive detection of aflatoxin b1," *Analytical Chemistry*, vol. 91, no. 1, pp. 1194–1202, 2019.

[5] A. Mertelj, B. Lampret, D. Lisjak, J. Klepp, J. Kohlbrecher, and M. Čopič, "Evolution of nematic and ferromagnetic ordering

in suspensions of magnetic nanoplatelets," *Soft Matter*, vol. 15, no. 27, pp. 5412–5420, 2019.

[6] A. V. Sandulyak, D. A. Samdulyak, V. A. Ershova, M. N. Polismakova, and N. Pamme, "Suspension temperature as a rheological control parameter in magnetic separation," *Glass and Ceramics*, vol. 77, no. 7-8, pp. 318–321, 2020.

[7] A. G. Boitsov, M. V. Siluyanova, S. V. Kurilovich, and V. V. Kuritsyna, "Applicability of magnetic abrasive machining by means of diamond suspensions in gas-turbine production," *Russian Engineering Research*, vol. 40, no. 8, pp. 692–695, 2020.

[8] Y. Fujii, J. Asama, T. Oiwa, and A. Chiba, "Positioning accuracy improvement for a magnetically levitated system using zero-sequence current of a permanent magnet motor," *IEEE Transactions on Industry Applications*, vol. 139, no. 3, pp. 322–329, 2019.

[9] C. Luo, K. Zhang, W. Zhang, and Y. Jing, "3d analytical model of permanent magnet and electromagnetic hybrid halbach array electrodynamic suspension system," *Journal of Electrical Engineering & Technology*, vol. 15, no. 4, pp. 1713–1721, 2020.

[10] J. Tang, X. Zhao, Y. Wang, and X. Cui, "Adaptive neural network control for rotor's stable suspension of vernier-gimballing magnetically suspended flywheel," *Proceedings of the Institution of Mechanical Engineers - Part I: Journal of Systems & Control Engineering*, vol. 233, no. 8, pp. 1017–1029, 2019.

[11] R. Kumar, S. Sood, C. Raju, and S. A. Shehzad, "Hydromagnetic unsteady slip stagnation flow of nanofluid with suspension of mixed bio-convection," *Propulsion and Power Research*, vol. 8, no. 4, pp. 362–372, 2019.

[12] E. Frishman, "The interaction forces in magnetic support systems of vertical type," *Communication Quarterly*, vol. 67, no. 3, pp. 614–618, 2019.

[13] Y. Yuan, Y. Ma, S. Guo, F. Yang, and B. Xu, "Suspension performance analysis of a novel bearingless motor," *Electronics Letters*, vol. 56, no. 3, pp. 132–134, 2020.

[14] C. S. Maurya and C. Sarkar, "Effect of Fe_3O_4 nanoparticles on magnetorheological properties of flake-shaped carbonyl iron water-based suspension," *IEEE Transactions on Magnetics*, vol. 56, no. 12, pp. 1–8, 2020.

[15] A. B. Meddeb, I. Chae, F. Scurti, J. Schwartz, S. H. Kim, and Z. Ounaies, "From a cholesteric non-aqueous cellulose nanocrystal suspension to a highly ordered film," *MRS Advances*, vol. 5, no. 64, pp. 3547–3554, 2020.

[16] O. F. Kandarakov, A. M. Demin, V. I. Popenko et al., "Factors affecting the labeling of nih 3t3 cells with magnetic nanoparticles," *Molecular Biology*, vol. 54, no. 1, pp. 99–110, 2020.

[17] E. N. Andreev, D. N. Arslanova, E. V. Akhmetzyanova et al., "Combined electromagnetic suspensions with reduced energy consumption for levitation vehicles," *Technical Physics*, vol. 64, no. 7, pp. 1060–1065, 2019.

[18] J. Qi, H. Lan, R. Liu, H. Liu, and J. Qu, "Efficient microcystis aeruginosa removal by moderate photocatalysis-enhanced coagulation with magnetic zn-doped fe_3o_4 particles," *Water Research*, vol. 171, no. Mar.15, pp. 115448.1–115448.8, 2020.

[19] H. Arya, M. M. Sarafraz, and M. Arjomandi, "Pool boiling under the magnetic environment: experimental study on the role of magnetism in particulate fouling and bubbling of iron oxide/ethylene glycol nano-suspension," *Heat and Mass Transfer*, vol. 55, no. 1, pp. 119–132, 2019.

[20] H. Zhu and T. Liu, "Rotor displacement self-sensing modeling of six-pole radial hybrid magnetic bearing using improved particle swarm optimization support vector machine," *IEEE Transactions on Power Electronics*, vol. 35, no. 11, pp. 12296–12306, 2020.